BIOCHEMICAL AND BIOPHYSICAL RESEARCH COMMUNICATIONS **229,** 176–181 (1996)
ARTICLE NO. 1776

Self-Assembly of the Brain MAP-2 Microtubule-Binding Region into Polymeric Structures Resembling Alzheimer Filaments

Edith Yi Zhang,* Michael A. DeTure,* Michael R. Bubb,† Tamara L. Caviston,* Gregory W. Erdos,‡ Scott D. Whittaker,‡ and Daniel L. Purich*,[1]

**Department of Biochemistry & Molecular Biology and †Department of Medicine, College of Medicine, and the ‡Interdisciplinary Center for Biotechnology Research, University of Florida, Gainesville, Florida 32610-0245*

Received October 7, 1996

The neuronal microtubule-associated protein known as MAP-2 has not been considered to be a subunit of paired helical filaments (PHFs) in neurofibrillary tangles seen in Alzheimer's Disease. We now describe the assembly of paired helical filament-like structures from MAP-2's 203-residue microtubule-binding region (MTBR). SDS gel electrophoresis and equilibrium ultracentrifugation suggest that a dimeric form, cross-linked by an interchain disulfide, is involved in polymerization. MAP-2 MTBR polymers bind thioflavin-S, a dye used to histochemically localize Alzheimer neurofibrillary tangles. Our finding that PHF-like structures assemble from a MAP-2 fragment raises new questions about MAP-2's role in the etiology of Alzheimer's Disease.

Neurofibrillary tangles, the supramolecular aggregates found in autopsy brain of Alzheimer patients (1-2), are formed from paired helical filaments (3-5). The microtubule-associated protein known as tau protein is thought to be the principal building-block of straight filaments and paired helical filaments (2,6,7). The closely related brain cytomatrix component MAP-2 also stabilizes microtubules (8). Tau predominates in adult axons, and MAP-2a and MAP-2b are found in dendrites and perikaryal regions. MAP-2 cross-links MTs to one another as well as to microfilaments, intermediate filaments, and vesicles (8-11). Several non-identical 31-amino acid repeats form a shared structural motif in tau and MAP-2, and synthetic repeat peptide analogues promote tubulin polymerization (12,13) and block MAP-2 binding to MTs (14). MAP-2 antibodies react with NFTs in autopsy brain tissue from AD patients (15-17), but the role of MAP-2 in the formation of NFTs remains uncertain. Tau's MTBR-K12 fragment can directly form paired helical filament-like structures (18), and this tau fragment contains the sequence repeats also present in the MAP-2 microtubule-binding region. We now demonstrate that a 203-residue MAP-2 microtubule binding region readily self-assembles *in vitro* to form polymeric structures resembling pronase-treated paired helical filaments observed in Alzheimer's Disease.

EXPERIMENTAL PROCEDURES

Bovine MAP-2 MTBR fragment, expressed and purified as described elsewhere (19,20), was dialyzed against 100 volumes of 100 mM Tris-HCl (pH 6.8), with three buffer changes for 6-9 hours; samples were then concentrated to 12-18 mg/ml using Amicon Centriprep concentrators at room temperature. The buffer was changed to 0.2 M Tris-0.2 M sodium acetate (pH 6.8) by diluting with 0.6 M Tris-HCl and 1.0 M sodium acetate at the same pH. Aliquots (20 μl) were placed in sitting-bridge crystallization cells (Hamilton Research, Inc., Laguna Hills, CA) and kept at room

[1] Address inquiries to: D. L. Purich, Department of Biochemistry & Molecular Biology, University of Florida College of Medicine [E-Mail: dlpurich@biochem.med.ufl.edu].

Abbreviations: PHF, paired helical filament; NFT, neurofibrillary tangle; MAP, microtubule-associated protein; MT, microtubule; MTBR, microtubule binding region.

0006-291X/96 $18.00

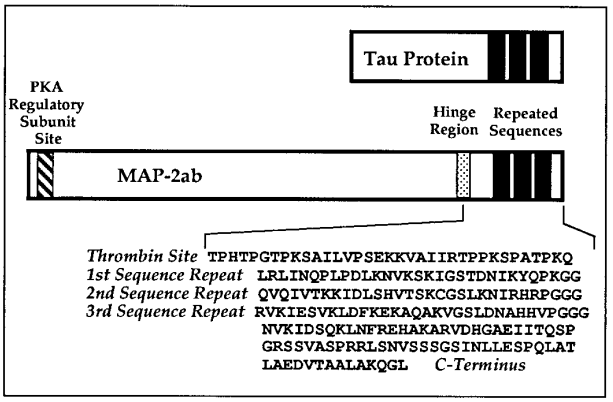

FIG. 1. Structural organization of MAP-2 and tau protein. In this diagram, the sequence of MAP-2 MTBR is aligned with respect to the repeated sequences, each ending in PXGG.

temperature for 1 day to 3 weeks in a sealed vapor equilibration chamber containing 1 ml 0.6 M Tris-HCl (pH 6.8) with 1M sodium acetate. Samples were added to carbon-coated 400 mesh copper grids for 30 s, followed by negatively staining with 1-2% uranyl acetate for 30 s. Grids were examined on a Hitachi H-7000 electron microscope at 75 kV. We used 12.5 percent cross-linked polyacrylamide gels with 0.1% SDS. Sedimentation runs were made in the Beckman XLA analytical ultracentrifuge (21), and data were collected at 0.003 cm increments at 280 nm. Equilibrium was attained when no changes were noted during a 24h interval. Thioflavin-S binding to MAP-2 MTBR polymers was monitored by the change of extrinsic fluorescence using a Photon Technology International Model A1010 photon-counting spectrofluorimeter.

RESULTS

Although they have structurally unrelated projection-arms, tau protein and MAP-2 have microtubule-binding regions that closely resemble each other (Fig. 1). Our 203-residue MTBR fragment is 81 residues longer than tau K12 fragment, and both fragments contain a single sulfhydryl group in their repeated sequence motifs. Because cysteine oxidation in K12 is required for polymerization (18), we adopted conditions favoring thiol group oxidation. Although no filaments could be detected during the first two weeks, the MAP-2 MTBR samples became viscous within the first few days. Electron microscopy confirmed the massive formation of long filamentous structures formed after 17-18 days. As shown in Figs. 2B-D, these polymers have a uniform diameter indicative of a regularly spaced substructure. They are also similar in size and appearance to pronase-treated PHF cores isolated from autopsy brain of Alzheimer patients (6). The average polymer length of 0.22 μmeters is probably an underestimate, because mechanical shearing may have occurred during preparation for electron microscopy.

Schweers *et al.* (18) found that the K12 fragment dimerized, and we characterized the dimerization of MAP-2 MTBR under conditions favoring its polymerization. We first used sodium dodecyl sulfate gel electrophoresis in the absence of reducing agent (Fig. 3A); extensive dimerization occurred even in the first day (Lane 1) and persisted for 3 weeks (Lanes 2-8). When the day-20 sample was treated with dithiothreitol (12.5 mM) at 90°C for 5 min, SDS electrophoresis confirmed that the dimer was reconverted to monomer (Lane 9). With only one thiol per MAP-2 fragment, MTBR dimerization is necessary to form a disulfide bond, and we employed sedimentation equilibrium ultracentrifugation to study the MTBR fragment in the absence and presence of dithiothreitol. Sedimentation equilibrium was attained after about one day, and no change in the protein concentration gradient was subsequently detected over a five-day run. The MAP-2 MTBR fragment formed about 32% dimer in the absence of the

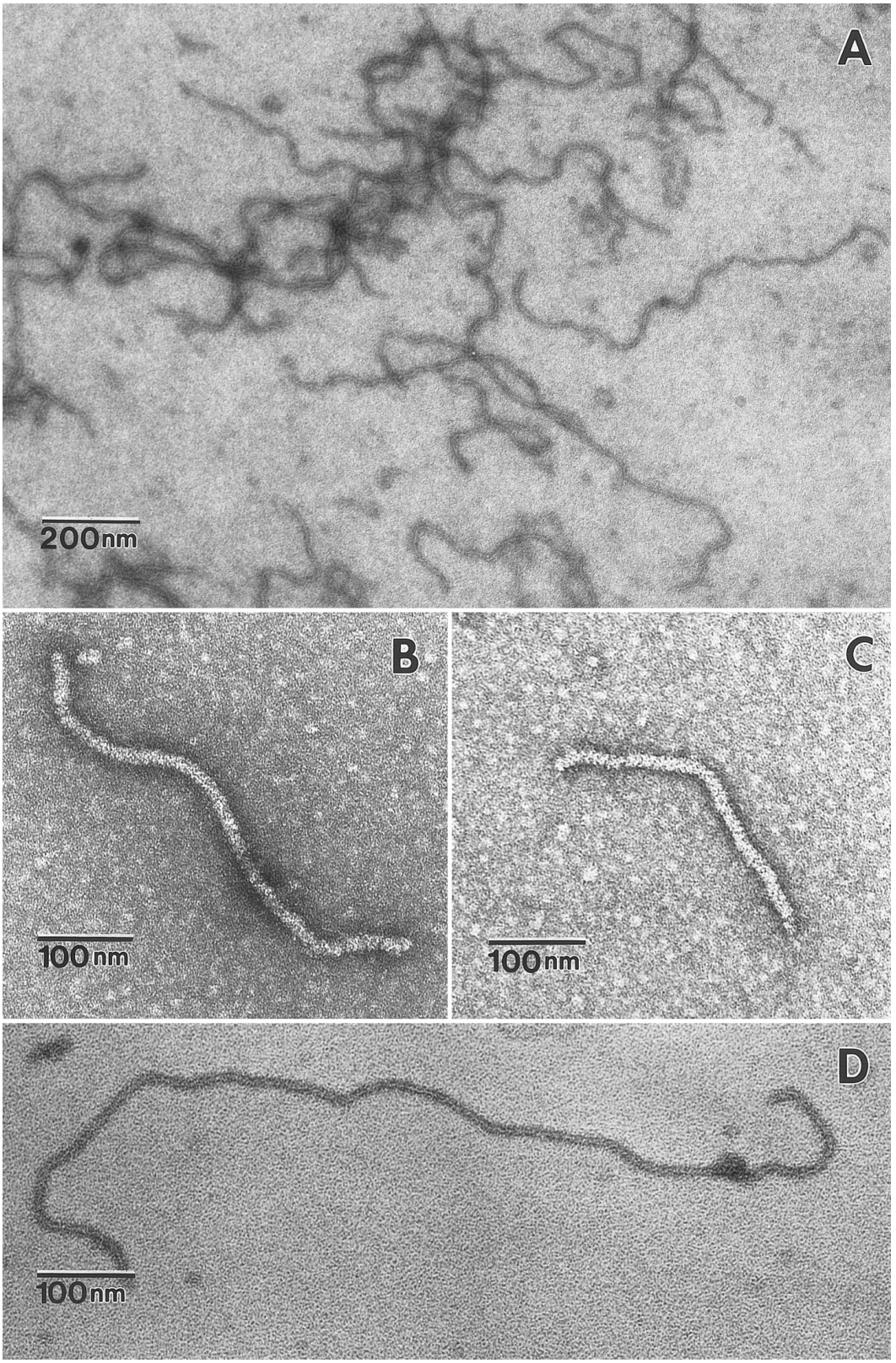
A
200nm
B
100nm
C
100nm
D
100nm

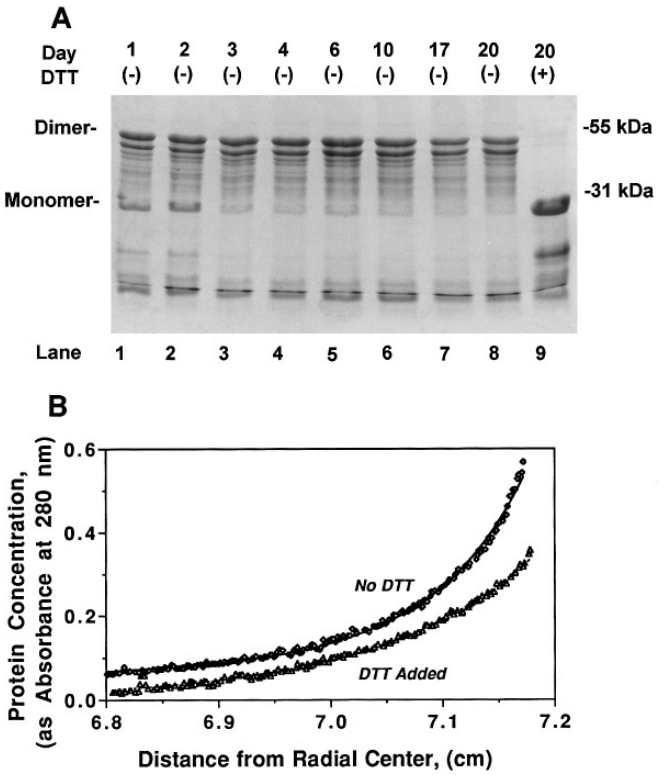

FIG. 3. A, SDS Gel electrophoresis of MAP-2 MTBR. Samples were incubated for the indicated times. A day-20 sample (Lane 9) was treated with dithiothreitol prior to electrophoresis. The molecular weights indicated at the right correspond to mobilities of carbonic anhydrase (31 kDa) and glutamate dehydrogenase (55 kDa). [Note: The 22 kDa MAP-2 MTBR is known to migrate as though its molecular weight is 28 kDa. The combinatorics of pair-wise dimerization of the monomer and its lower molecular weight fragments account for the manifold of minor dimer bands appearing below the major dimer band.] B, Sedimentation equilibrium behavior of MAP-2 MTBR. The observed protein concentration gradients were analyzed using a monomer molecular weight of 22,004. Best fit theoretical curves, generated with a rapid equilibrium monomer–dimer model, are included. After treatment with dithiothreitol to reduce interchain disulfide linkages, the data in the lower curve fit a single exponential for monomer only.

reducing agent (Fig. 3B), and little or no dimer could be detected in the presence of dithiothreitol. Neurofibrillary tangles bind thioflavin-S and Congo red, and this has become a clinically useful property in the diagnosis of Alzheimer's disease (22,23). Tau K12 polymers bind these aromatic dyes (18), and we carried out fluorescence binding experiments using thioflavin-S. As shown in Fig. 4, thioflavin-S binding to MAP-2 MTBR was clearly evidenced by the characteristic fluorescence enhancement with assembled filaments. Amyloid fibers, formed by assembly of Aβ peptide, and PHFs have a so-called cross-β structure allowing them to interact with thioflavin-S. Our data suggest that some similar dye-binding pocket is created during the polymerization of MAP-2 MTBR. Finally, the filament protein concentrations used in these

FIG. 2. Electron micrographs of polymerized MAP-2 MTBR. A, Low magnification image showing masses of polymerized filaments; B-D, Selected fields of polymerized MAP-2 MTBR. Note that the assembled structures are of uniform diameter, estimated to be about 12 nm based on the magnifications used.

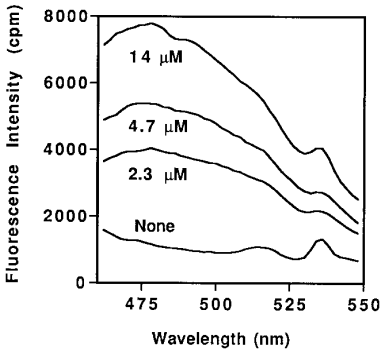

FIG. 4. Thioflavin-S binding to polymerized MAP-2 MTBR. The excitation wavelength was set at 440 nm and the emission spectra were recorded from 460 to 550 nm. Spectra were taken with the dye and assembled polymer (corresponding to total MAP-2 MTBR monomer concentrations of 0, 2.3, 4.7, and 14 μM).

fluorescence measurements were 30-100 times lower than that used during assembly, and electron microscopy verified the stability of the polymeric structures even after such dilution.

DISCUSSION

Our work indicates that polymers of MAP-2 microtubule-binding region resemble straight filament regions of PHFs, and we have reproducibly found filaments in several hundred individual runs. This finding invites consideration that MAP-2, or a proteolytic fragment derived from this neuronal cytomatrix protein, may factor into the genesis of NFTs in Alzheimer's disease. The core structure of Alzheimer PHFs is thought to be made up of tau protein or its fragments (6), but tau may not be the single, exclusive subunit of paired helical filaments (24). Earlier workers (15-17) observed that antibodies against MAP-2-specific epitopes bind to NFTs in autopsy brain tissue from AD patients, and a monoclonal antibody to MAP-2 prominently stained NFTs in the most affected areas of AD brain (15). Polyclonal anti-MAP-2 antibodies stained abnormal neurites around senile plaque (16). Such observations are now strengthened by our findings, but a role for MAP-2 in neurofibrillary tangle formation still remains conjectural.

Alzheimer-like filament assembly from full-length tau protein has been clearly demonstrated (25,26). Structural cues permitting tau to form PHFs may be absent in MAP-2, thereby blocking intracellular formation and/or accumulation of intact MAP-2 in PHFs. MAP-2 is, however, remarkably susceptible to limited proteolysis (13, 27), with cleavage occurring preferentially in the hinge region between the projection-arm and MTBR. (see Fig. 1). The MTBR fragment used in this work can be generated by thrombin cleavage of MAP-2ab (13), and there are also trypsin and chymotrypsin cleavage sites within the hinge region (27,28). Aberrant action of these and related proteases within neurons could generate fragments capable of forming PHFs or of influencing the minimal concentration of tau required for PHF assembly. Nevertheless, the findings reported in this communication should now refocus attention on MAP-2's potential role in the pathobiology of Alzheimer Disease so that definitive conclusions can be reached.

REFERENCES

1. Anderton, B. H. (1993) *Hippocampus* **3,** 227–237.
2. Trojanowski, J. Q., and Lee, V. M. (1994) *Am. J. Pathol.* **144,** 449–453.
3. Kidd, M. (1963) *Nature* **197,** 192–193.
4. Terry, R. D. (1963) *J. Neuropath. Exp. Neurol.* **22,** 629–642.
5. Wisniewski, H. M., Narang, H. K., and Terry, R. D. (1976) *J. Neurol. Sci.* **27,** 173–181.
6. Wischik, C. M., Novak, M., Thorgersen, H. C., Edwards, P. C., Runswick, M. J., Jakes, R., Walker, J. E., Milstein, C., Roth, M., and Klug, A. (1988) *Proc. Natl. Acad. Sci.* **85,** 4506–4510.

7. Wood, J. G., Mirra, S. S., Pollack, N. J., and Binder, L. I. (1986) *Proc. Natl. Acad. Sci.* **83,** 4040–4043.
8. Purich, D. L., and Angelastro, J. M. (1994) *Adv. Enzymol.* **69,** 121–154.
9. Hirokawa, N. (1982) *J. Cell Biol.* **94,** 129–142.
10. Hirokawa, N., Hisanga, S., and Shiomura (1988) *J. Neurosci.* **8,** 2769–2779.
11. Leterrier, J.-F., Liem, R. K. H., and Shelanski, M. L. (1982) *J. Cell Biol.* **95,** 982–986.
12. Ennulat, D. J., Liem, R. K. H., Hashim, G. A., and Shelanski, M. L. (1989) *J. Biol. Chem.* **264,** 5327–5330.
13. Joly, J. C., Flynn, G., and Purich, D. L. (1989) *J. Cell Biol.* **109,** 2289–2294.
14. Joly, J. C., and Purich, D. L. (1990) *Biochem.* **29,** 8916–8920.
15. Kosik, K. S., Duffy, L. K., Dowling, M. M., Abraham, C., McCluskey, A., and Selkoe, D. J. (1984) *Proc. Natl. Acad. Sci.* **81,** 7941–7945.
16. Dammerman, M., Yen, S., and Shafit-Zagardo, B. (1989) *J. Neurosci. Res.* **24,** 487–495.
17. Nukina, N., and Ihara, Y. (1983) *Proc. Japan Acad.* **59,** 284–292.
18. Schweers, O., Mandelkow, M., Biernat, J., and Mandelkow, E. (1995) *Proc. Natl. Acad. Sci.* **92,** 8463–8467.
19. Ainsztein, A. M., and Purich, D. L. (1994) *J. Biol. Chem.* **45,** 28465–28471.
20. Coffey, R. L., Joly, J. C., Cain, B. D., and Purich, D. L. (1994) *Biochemistry* **33,** 13199–13207.
21. Bubb, M. R., Lewis, M. S., and Korn, E. D. (1991) *J. Biol. Chem.* **266,** 3820–3826.
22. Inouye, H., Fraser, P. E., and Kirschner, D. A. (1993) *Biophys. J.* **64,** 502–519.
23. LeVine, H. (1993) *Protein, Sci.* **2,** 404–410.
24. Wischik, C. M., Harrington, C. R., Lai, R. Y. K., Mukaetova-Ladinska, E. B., Xuereb, J. H., Gertz, H., Wischik, D. J., Edwards, P. C., Mena, R., and Roth, M. (1995) *Neurobiol. of Aging* **16,** 423–431.
25. Crowther, R. A., Olesen, O. F., Smith, M. J., Jakes, R., and Goedert, J. M. (1994) *FEBS Lett.* **337,** 135–138.
26. Wilson, D. M., and Binder, L. I. (1995) *J. Biol. Chem.* **270,** 24306–24314.
27. Vallee, R. B., and Borisy, G. G. (1980) *J. Biol. Chem.* **252,** 377–382.
28. Dingus, J., Obar, R. A., Hyams, J. S., Goedert, M., and Vallee, R. B. (1991) *J. Biol. Chem.* **266,** 18854–18860.